JLU
NEUE WEGE. SEIT 1607.

JUSTUS-LIEBIG-
UNIVERSITÄT
GIESSEN

IIPI
Experimental Physics II

LCR
Laboratory Course Report

High-altitude balloon experiment

Implementation of a nuclear photo emulsion for the detection of high-energy particles in cosmic radiation.

William Roster

Matr. Nr.: 1115493
Summer Semester 2020

II. Physics Institute [Subatomic particle physics]
Group : Apl. Prof. Dr. Jens Sören Lange
FB 07

Justus-Liebig University Giessen &
Technische Hochschule Mittelhessen - University of Applied Sciences
Heinrich-Buff-Ring 16
Campus: Natural Sciences
35392 Giessen, Germany

Giessen, 2020

Contact: william.t.roster@physik.uni-giessen.de

Contents

CHAPTER 1

Introduction

Going into space is going into the great unknown. It is vast, hostile and seemingly very far away. However, now more than ever, space is also accessible. Contrary to the expected, this applies to even the most basic individuals with the necessary know how. Roughly 50 years ago, humans first took to dimensions no longer describable with aerodynamics but rather by the laws of astrodynamics. Today even space-enthusiastic self-taught amateurs are able to conduct scientific research in heights of over 30 km above earth.
This is made possible by so-called "high-altitude balloon" (HAB) missions. These balloons carry probes equipped with digital cameras, filming the ascent, and GPS localization trackers used for the retrieval of the probe. The recordings of the earth made in this way are both impressive and valuable due to the obtained information content. They represent a significantly simplified, but nevertheless in many ways comparable approach to satellite missions. Consequently HAB-missions serve as ideal substitute for cost-intensive satellite missions, as they prove to be a reliable alternative for testing new methods and technologies.
Not only the aspect of independent exploration of the earth's atmosphere and its components, but the high altitude regions into which HAB's penetrate, is of particular interest. Planes bound to atmospheric layers with higher pressure (up to 10 kilometers) and satellites to orbits in layers with hardly any pressure (as of 200 kilometers), clarify the difficulty and challenge of performing extensive research in this atmospheric gap. The scientific events taking place, motivated by the magnetic field or the atmospheric molecules themselves for example, are only explorable with either sounding rockets or HAB-missions.

One such effect is the spallation of the high-energy protons contained within cosmic radiation, when they collide with the atomic nuclei of particles in the denser layers of the atmosphere, thus resulting in secondary radiation. The reactions of the primary radiation initially produce pions and, to a lesser extent, kaons. These then decay due to the weak interaction, creating muons and muon neutrinos. At sea level, the particle flux density of these "cosmic" muons is around $100/m^2s$.
However the detection of muons on the earth's surface is not as straight forward as it may initially appear. This is because muons would long have decayed before reaching the surface if it was not for the effects of time dilation and length concentration. These phenomena are obviously linked to Albert Einstein's theory of general

relativity and the muons moving at velocities close to the speed of light. As the presence of muons on the earth's surface can be seen as indirect evidence for the presence of kaons in the atmosphere, this experiment aims to capture such an event. In order to do so, the probe will be fitted with a photosensitive chemical suspension. If the suspension is struck by particles of a certain wavelength, stripe patterns emerge as the embedded halides start to perform crystallization and align to create an ion lattice. Based on the the width of the recorded stripes, the reaction can be traced back to the according particle.

The following chapters give a more detailed particle physics approach regarding the science of kaons, as well as an overview portraying the factors which need to be taken into account when building and flying the HAB. This way, the report can be seen as a guidebook for scientific and administrative actions taken. Finally the research data will be analysed and evaluated.

CHAPTER 2

Cosmic radiation

Great mysteries of the universe surround earth, all the time. One such mystery is cosmic rays, which in general, are atom fragments which continuously rain down on the Earth from outside of the solar system. Some carry so much energy that it remains unclear what object in the universe could have created them. Many are much too powerful to have originated from the sun. Some are even much too powerful to have originated from an exploding star.[**1**][**2**]
This is why they are categorized into two major groups:

- **galactic cosmic rays (GCR)**, i.e., high-energy particles originating outside the solar system
- **solar energetic particles**, high-energy particles emitted by the sun, primarily in solar eruptions

The sources of these rays, as well as the effect of astroparticles colliding with the upper layers of earth's atmosphere, will be elucidated in this chapter. With the HAB-mission in mind, a corresponding measurement process for particle detection, will also be presented.

2.1 Component properties

In 1909, the german physicist Theodor Wulf developed an electrometer, a device to measure the rate of ion production inside a hermetically sealed container, and used it to show higher levels of radiation at the top of the Eiffel Tower than at its base. However the majority of the public declined these measurements and his theory. So did Victor Hess, who carried three enhanced-accuracy Wulf electrometers to an altitude of 5,300 metres in a free balloon flight in 1912. With the initial plan of isolating his experiment from radiation in advanced altitudes, he found the ionization rate increased approximately by a factor of 4 over the rate at ground level. Hess ruled out the Sun as the radiation's source by making a balloon ascent during a near-total eclipse. With the moon blocking much of the Sun's visible radiation, Hess still measured rising radiation at rising altitudes.
He concluded that: *"The results of the observations seem most likely to be explained by the assumption that radiation of very high penetrating power enters from above into our atmosphere."*, winning him the 1936 Nobel prize in physics.[**3**]

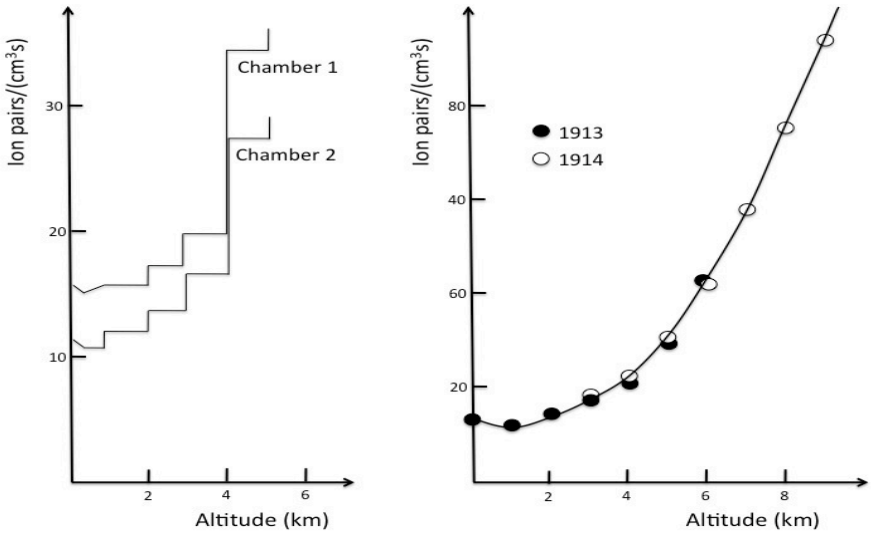

Figure 2.1: Graph showing the increase of ionization with altitude as measured by Hess in 1912 (left) and by Kolhörster (right) Credit: Springer.

Although the name would suggest that cosmic rays are some form of electromagnetic radiation, they are actually subatomic particles travelling at significant fractions of the speed of light. As mentioned at the beginning of the chapter, cosmic rays are an ionizing radiation consisting of high-energy protons, α particles and atomic nuclei which move through space at nearly the speed of light. They originate from outside of the solar system and from distant galaxies. A second source of cosmic radiation is the release of charged particles from the sun, which become significant during periods of solar flare. All of the natural elements in the periodic table are present in cosmic rays. This includes elements lighter than iron, which are produced in stars, and heavier elements that are produced in more violent conditions. The amount of cosmic radiation that reaches the earth from the sun and outer space varies. Its energy is effectively absorbed by the atmosphere and is also affected by the earth's magnetic field, which is why natural phenomena such as the northern lights become visible. Since cosmic rays are charged – positively charged protons or nuclei, or negatively charged electrons – their paths through space can be deflected by magnetic fields. On their journey to Earth, the magnetic fields of the galaxy, the solar system, and the Earth scramble their flight paths so much that one can no longer know exactly where they came from. This is illustrated in Fig. 2.2. This ultimately means that their origin needs to be determined by indirect methods. Such methods include the investigation and analysis of the spectroscopic signature each nucleus gives off in radiation, and also by weighing the different isotopes of elements which struck particle detectors similar to those used in nuclear and high-energy physics. Direct measurement of cosmic rays has become possible since the launch of the first satellites in the late 1950s.[**4**][**5**]

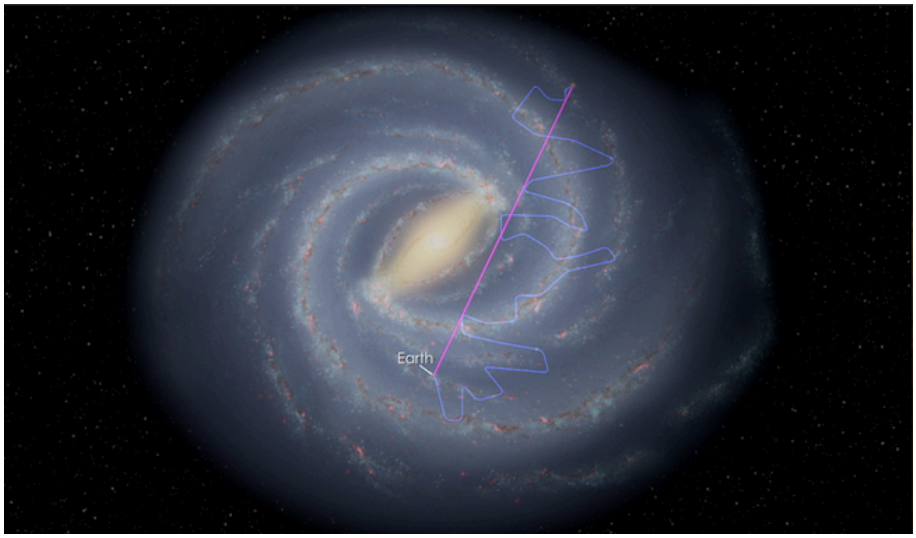

Figure 2.2: Illustration of the scrambled path taken by particles reaching earth, as shown by the blue path. Light (photons) however travels in a straight line, as shown by the purple path. This makes the detection and trace-back of the origin much easier. Credit: NASA's Goddard Space Flight Center.

2.1.1 Sources of energy

Cosmic rays attract great interest practically, due to the damage they inflict on microelectronics and life outside the protection of an atmosphere and magnetic field, and scientifically, because the energies of the most energetic ultra-high-energy cosmic rays (UHECRs) have been observed to approach 3×10^{20} eV, about 40 million times the energy of particles accelerated by the Large Hadron Collider (LHC). One can show that such enormous energies might be achieved by means of the centrifugal mechanism of acceleration in active galactic nuclei (AGN). At 50 J, the highest-energy ultra-high-energy cosmic rays, such as the Oh-My-God particle recorded in 1991, have energies comparable to the kinetic energy of a formula 1 car moving at 1 $\frac{km}{h}$. As a result of these discoveries, there has been interest in investigating cosmic rays of even greater energies. Most cosmic rays, however, do not have such extreme energies. The energy distribution of cosmic rays peaks at about 0.3 GeV (4.8×10^{-11} J).[**6**][**7**]
Most galactic cosmic rays are probably accelerated in the blast waves of supernova remnants. The remnants of the explosions – expanding clouds of gas and magnetic field – can last for thousands of years, and this is where cosmic rays are accelerated. Bouncing back and forth in the magnetic field of the remnant randomly lets some of the particles gain energy, and become cosmic rays. Eventually they build up enough speed that the remnant can no longer contain them, and they escape into the galaxy.

Extensive air showers (EAS) produced when a UHECR interacts with an air nucleus in the upper atmosphere have been measured since their discovery by Pierre Auger in the 1930s. Data from the Fermi Space Telescope (FST) has been interpreted as evidence that a significant fraction of primary cosmic rays originate from the supernova explosions of stars. AGN also appear to produce cosmic rays, based on observations of neutrinos and gamma rays from blazar TXS 0506+056 in 2018.[**8**]

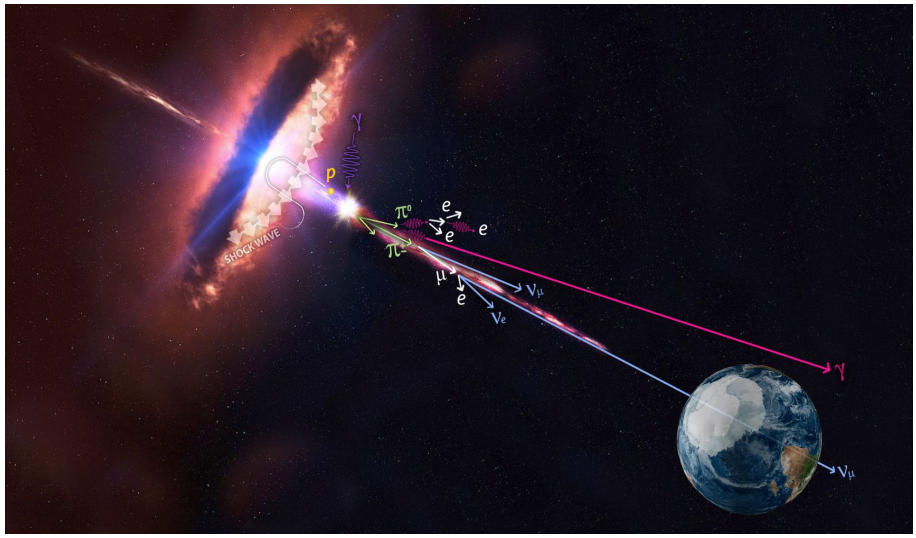

Figure 2.3: Artists illustration of galactic cosmic rays creation. AGN jet streams accrete particles which are energized in a shock wave. Highly-energetic particles are long living and therefore travel great distances before reaching earth. Credit: Space.com.

2.1.2 Earth's atmosphere

The earth's atmosphere (from the Greek atmos: haze, and sphaira: sphere) is understood as the gaseous envelope around the earth's surface. In addition to the force of attraction, it is also subject to inertial forces such as the Coriolis force, which result from the rotation of the earth. In addition, there are convective forces which result from differences in density. The interplay of all forces is responsible for the dynamics of the atmosphere and thus for the weather and climate events. The atmosphere has a mass of around 5 quadrillion tons. The mean pressure of 1013 hectopascals on the earth's surface, together with the corresponding temperatures, makes it possible for water to exist on earth in a liquid state and for life as we know it to be possible. The earth's atmosphere chemically consists of 78% nitrogen (N_2), 20% oxygen (O_2) and 1% a mixture of argon (Ar), carbon dioxide (CO_2) and hydrogen up to an altitude

of around 80-90 km (H_2) and other gases. This layer with a relatively constant composition is also called the "homosphere". Above that, gases with a lower density, like Helium or Hydrogen, predominantly occur.[**9**]

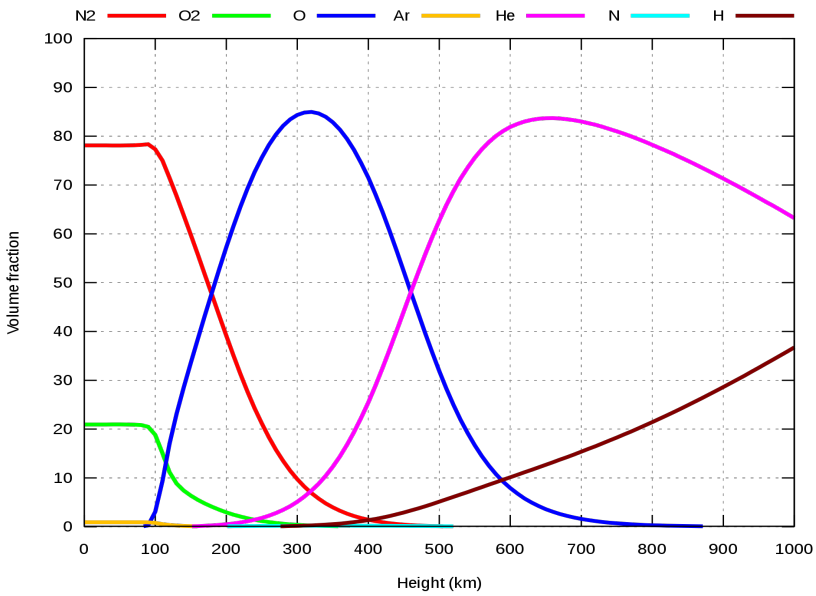

Figure 2.4: The volume fraction of the main constituents of the Earth's atmosphere as a function of height according to the MSIS-E-90 atmospheric model. Credit: Space.stackexchange.com.

The atmosphere is divided into different layers according to its temperature profile. Therefore the lowest layer of the atmosphere, the troposphere, extends from the earth's surface to around 7 km above the poles and 17 km above the equator. In summer, this part of the earth's atmosphere, also known as the weather layer, is thicker than in winter due to thermal expansion. It contains 99% of the water vapor and 90% of the mass of the atmosphere. This means that almost all of the air is in the lowest layer of the atmosphere, which is only about 15 km thick. The properties of the air in this layer are determined by temperature, humidity, cloud cover, precipitation, air pressure, wind direction and strength. Weather balloons play an important role in determining these parameters. The knowledge of these physical quantities enables meteorologists to create weather forecasts and climate scenarios. The top of the troposphere is limited by the so-called tropopause. As an inversion layer, it is characterized by the fact that the air temperature slowly increases again from this altitude. It mediates the transition to the stratosphere above. This layer, in which the ozone layer is located, reaches up to a height of 50 km and is delimited by the stratopause.[**10**]

This is followed by the mesosphere, which ends at an altitude of around 80 km at the mesopause. The particle density of the subsequent thermosphere, which reaches up to an altitude of around 800 km, is already so low that in space travel "real space" starts from an altitude of roughly 100 km. That this is not completely correct can also be seen from the fact that near-earth satellites, such as the international space station (ISS), are slowed down in their orbital speed by the weak but still existing residual atmosphere. The exosphere forms the outermost layer of the earth's atmosphere (up to 10,000 km) and thus represents the transition to the vacuum of space.[**11**][**12**]

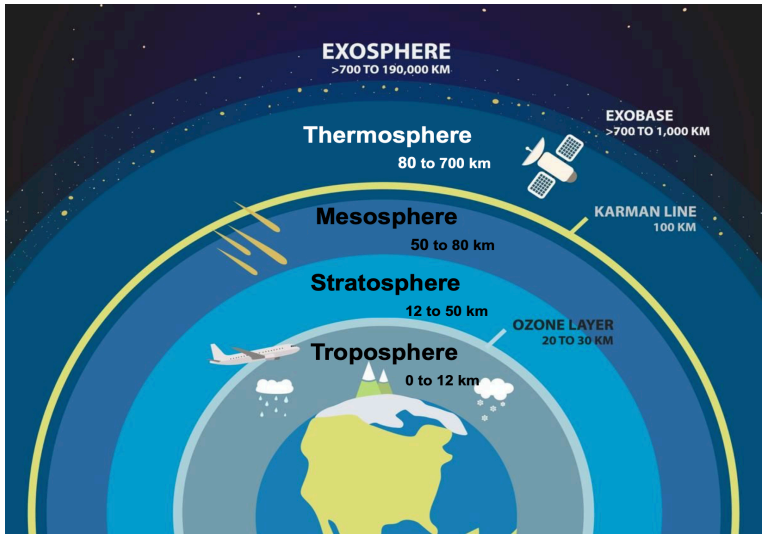

Figure 2.5: Earth's atmosphere and the individual layers which differ in temperature and pressure. Cosmic radiation showers as well as HAB-missions focus predominantly on the stratosphere. Credit: Pinterest.

As a rough approximation, the temperature in the lower atmosphere decreases linearly with altitude near the ground. The average temperature decreases about 5 - 7 K per kilometer in altitude. This inversion layer forms a natural barrier at which the weather normally ends. In this cold boundary layer, temperatures of around -55 °C are fairly constant. In contrast, the temperature in the stratosphere - with a significantly lower particle density - increases again to around 0 °C. The rise in temperature can primarily be attributed to processes in the ozone layer, which is located at a height of about 25 km, which in particular absorbs the short-wave, high-energy components of the sun's UV radiation and partially converts it into heat. [**13**]

2.2 Primary & secondary radiation

Of primary cosmic rays, which originate outside of Earth's atmosphere, about 99% are the nuclei of well-known atoms, stripped of their electron shells, and about 1% are solitary electrons, similar to beta particles. Of the nuclei, about 90% are simple protons, i.e., hydrogen nuclei. 9% are alpha particles, identical to helium nuclei and 1% are the nuclei of heavier elements, called HZE ions. These fractions vary highly over the energy range of cosmic rays. They are essential for the production of ^{14}C in our atmosphere, which is used in radiocarbon dating. A very small fraction are stable particles of antimatter, such as positrons or antiprotons. The precise nature of this remaining fraction is an area of active research. So far any attempts to detect anti-alpha particles have failed. Within cosmic-rays however one also finds other subatomic particles like neutrons, electrons and neutrinos. Among the products of these star explosions are gamma-ray photons, which (unlike cosmic rays) are not affected by magnetic fields. The gamma-rays studied had the same energy signature as subatomic particles called neutral pions. Pions are produced when protons get stuck in a magnetic field inside the shockwave of the supernova and crash into each other. The mass ratio of helium to hydrogen nuclei, 28%, is similar to the primordial elemental abundance ratio of these elements, 24%.

Fortunately, cosmic rays with energies greater than 10^{14} eV can be indirectly detected from the ground. Upon impact with the Earth's atmosphere, these cosmic rays interact with atoms, mainly oxygen and nitrogen, to produce secondary particles in a cosmic ray shower which sometimes reach the surface. It is then possible to determine the energy and direction of the original cosmic ray by studying the shower of particles.
The first interaction is when the high energy particles collide with nuclei in the upper atmosphere. They cause a 'spallation' reaction. A spallation reaction is a nuclear reaction where a highly energetic nucleon, usually a secondary cosmic-ray neutron of energy, collides with a target nucleus. This causes the release of multiple particles such as protons and neutrons. The accelerated particles cause a cascade of interactions in the upper atmosphere as they strike more atmospheric nuclei, creating additional particles and high energy radiation. The particles continue in the same direction, while photons are emitted in all directions. Cosmic radiation however is of no major significance at altitudes <25,000 feet (7620m) because of the attenuating properties of the earth's atmosphere.[**14**][**15**][**16**][**17**]

The cosmic ray cascade essentially has three components:

- The mesonic component
- The electromagnetic component
- The hadronic component

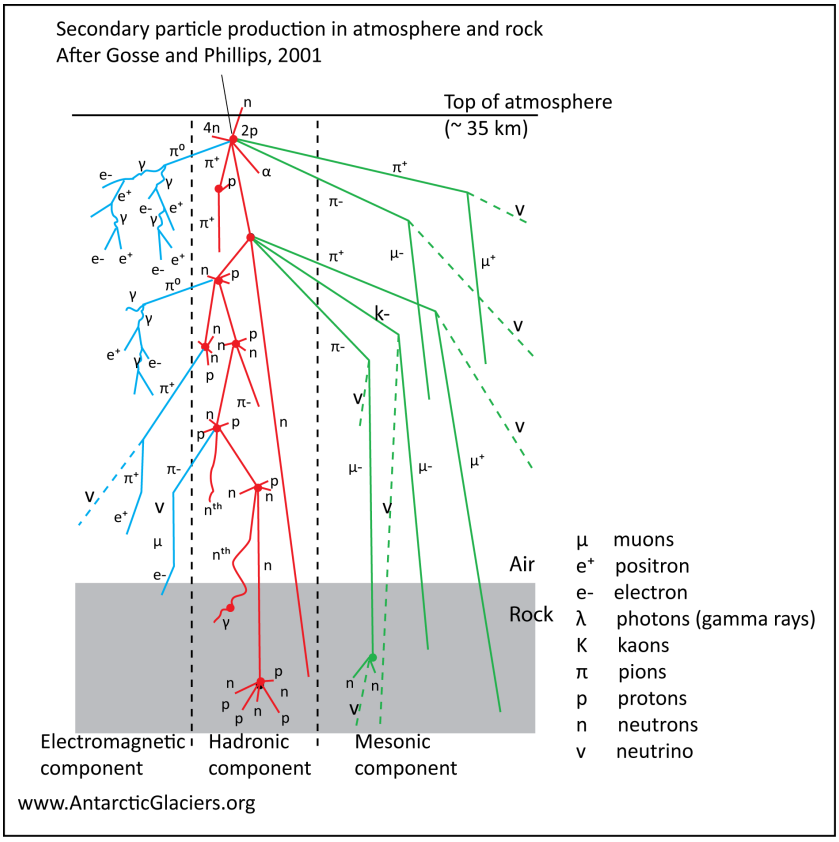

Figure 2.6: The cosmic ray cascade. Spallation reactions cause the formation of new cosmogenic nuclides in the atmosphere. Credit: Antarctic Glaciers.

The mesonic component consists of charged mesons such as positive or negative kaons (K) and pions (π) which degrade to muons (μ). Muons (mass 105.7 MeV/c^2), electrons (mass 0.511 MeV/c^2) and tau (mass 1777.8 MeV/c^2) are all leptons, which have no sub-structure and are not composed of simpler particles. A muon is about 2/3rds of the size of a proton or a neutron. They are unstable, lasting only a few hundredths of a microsecond. That being said, some high-energy muons even penetrate for some distance into shallow mines, and most neutrinos traverse the Earth without further interaction.

The second part of the primary interaction is the electromagnetic component, where the muons undergo further decay. When the cosmic ray collides with an atom, the sub-atomic pions (π) and kaons (K) produced, decay almost instantly to produce muons (μ) and photons (gamma rays) (γ). The muons and gamma rays then decay to form electrons (e^-) and positrons (e^+).[**18**]

The hadronic component comprises protons (p) and neutrons (n). A hadron is a composite particle made up of quarks held together by a strong force. Hadrons comprise baryons, such as protons and neutrons, and mesons. Protons and neutrons are stable. This component of the cosmic ray cascade is most important for cosmogenic nuclide dating. All of the secondary particles produced by the collision continue onward on paths within about 1° of the primary particle's original path.
After the shower maximum, more particles are stopped than created and the number of shower particles declines. Through successive interactions, energy is lost until the particles have insufficient energy to cause further spallation upon collision with another particle.

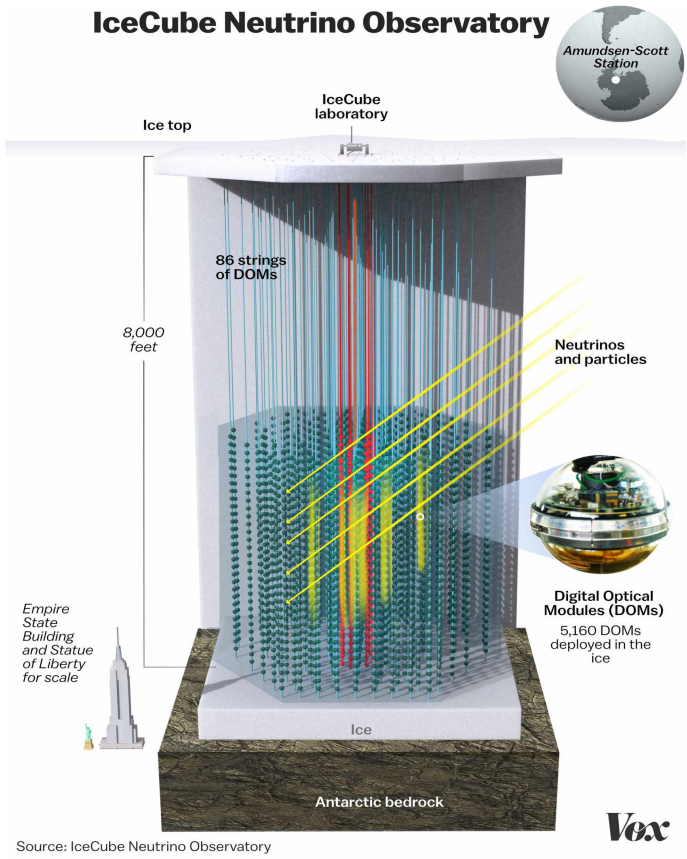

Figure 2.7: Neutrino detection observatory which is built below the surface of the south pole. Subatomic particle moving through ice exceed the speed of light creating Cherenkov radiation. Credit: IceCube Neutrino Observatory.

Of all secondary particles, subatomic particles called neutrinos display the highest event rate on the earth's surface. This is why, they serve as the basis in a few huge projects to better understand where cosmic rays come from. Neutrinos are different from the other components of cosmic rays in one really important way: They don't interact with other forms of matter much at all. They don't have any electrical charge. That means they travel through the universe in a relatively straight line. One involves a truly enormous block of ice at the South Pole. The IceCube Neutrino Observatory is a 1 km^3 block of crystal-clear ice surrounded by sensors. These sensors are set up to detect when neutrinos crash into Earth. Other known cosmic rays observatories are the Pierre Auger Observatory in Argentina and the scintillation & surface detectors in Utah, USA.[**8**]

2.3 Particle physics

Simply because most of the mass of an atom is concentrated in its nucleus, which is made up of baryons, scientists often use the term baryonic matter to describe so-called ordinary matter. This ordinary matter includes all accumulations of mass visible to mankind, meaning the definition is based on electromagnetic interactions. Ordinary matter commonly exists in four states: solid, liquid, gas, and plasma and is composed of two types of elementary particles: quarks and leptons. Protons and neutrons are both made up of quarks, where as electrons are categorised among the lightweight leptons [**19**][**20**].
In astronomical length scales, gravity is the dominant fundamental interaction as its effects are cumulative, unlike electromagnetism (EM), where positive and negative charges cancel each other out. As the two remaining interactions, the weak and the strong nuclear forces decline very rapidly with distance, their effects are confined mainly to sub-atomic length scales. As baryons consist of quarks, they succumb to all of the forces mentioned above, excluding EM if not charged. All known particles are officially categorized into groups of the same attributes using the so-called standard model of particle physics (see fig.2.8).
This model lists all so-far experimentally confirmed existing particles which compose matter. These are grouped in fermions and bosons, based on their spin. Furthermore fermions can be split into two collections, quarks and leptons, according to their electromagnetic charge. Within each collection the particles are ranked from left to right in mass. Corresponding "antimatter" partners as well as the force particles which mediate interactions by transferring energy are also listed. Such mediation particles, in particular the mass they carry, become significant when comparing the sum of a quark arrangement with the mass of the corresponding nucleus. Mediation particles are photons (γ) for electromagnetic interactions, gluon (g) for strong interaction and the gauge bosons Z^0, W^-, W^+ for weak interaction. However, the cause of the existence of the interactions could be traced back to the ambivalent symmetries. Due to this, particles of matter maintain a consistent appearance at all times and in all places.

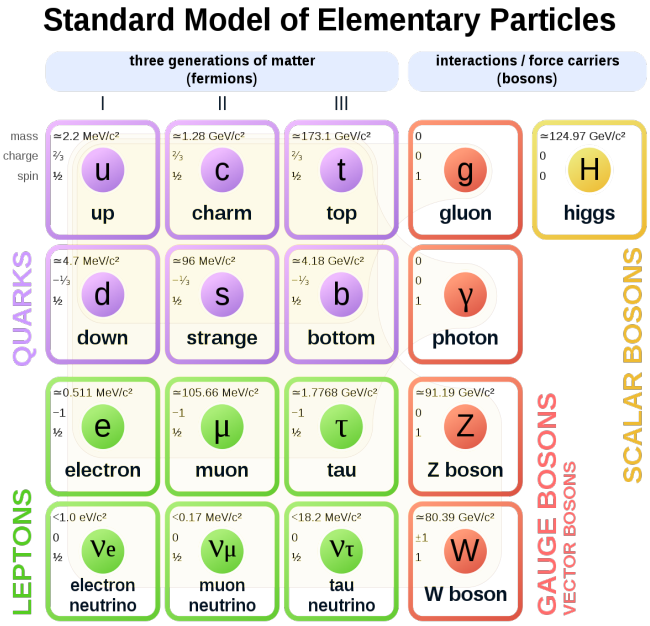

Figure 2.8: Standard model of elementary particles. This table contains all known and detected leptons, quarks and bosons as well as their characteristics to date. Credit: Quantumdiaries.

The standard model does not, however, accommodate gravity. A true force particle has not yet been attained. It can therefore not be a complete description of particle physics. Overall the universe appears to have much more matter than antimatter. This occurrence, also known as baryon asymmetry, is one of the most important phenomena of particle physics not yet understood, since it cannot be explained by the standard model of elementary physics. This imbalance between matter and antimatter is partially responsible for the existence of all matter existing today, since matter and antimatter, if equally produced at the Big Bang, would have completely annihilated each other and left only photons as a result of their interaction.[**21**]

2.4 Mesons

Hadronic subatomic particles such as Mesons compose of one quark and one antiquark, bound together by strong interactions. All mesons are unstable, with the longest-lived lasting for only a few hundredths of a microsecond. Charged mesons decay, either through mediating particles or directly in order to form electrons and neutrinos.

Uncharged mesons may decay to photons. Outside the nucleus, mesons appear in nature only as short-lived products of very high-energy collisions between particles made of quarks, such as cosmic rays with high-energy protons and neutrons. Mesons are defined simply as particles composed of an even number of quarks. Baryons on the other hand consist of at least 3 valence quarks and some experiments show evidence of exotic mesons, which do not have the conventional valence quark content of two quarks, but 4 or more.[**22**]
Because quarks have a spin $\frac{1}{2}$, the difference in quark number between mesons and baryons results in conventional two-quark mesons being bosons, whereas baryons are fermions. The different quark-antiquark arrangements and the corresponding meson types are listed in the table below where mesons are highlighted in green and antimesons in yellow. The qq combinations or *"Quarkonia (ss, cc, bb)"*, whose nomenclature follows the rules for mesons without flavor, are highlighted in white. The code letter of the meson is based on the heavier (anti-) quark: Depending on which is an s, c or b, the meson is called K, D or B. If the lighter (anti-) quark is not a u or d, it is also given as a lower index. For example: The combination *cs* is a D_s meson. The electrical charge Q is given as the upper index. If the heavier (anti-) quark is positively charged, it is by convention a meson, otherwise it is an antimeson. Electrically neutral antimesons are marked with a slash; this is not necessary for the electrically charged ones, since according to this convention, positively charged qq combinations are always mesons and negatively charged qq combinations are always antimesons.[**23**]

Meson arrangement					
Antiquark → Quark ↓	$\overline{down}$	$\overline{up}$	$\overline{strange}$	$\overline{charm}$	$\overline{bottom}$
down			K^0	D^-	B^0
up			K^+	$\overline{D^0}$	B^+
strange	$\overline{K^0}$	K^-		D_s^-	B_s^0
charm	D^+	D^0	D_s^+		B_c^+
bottom	$\overline{B^0}$	B^-	B_s^0	B_c^-	

Figure 2.9: Meson arrangement table representing every quark - antiquark combination including flavour and electrical charge notations. Credit: Futura-sciences.de.

Each type of meson has a corresponding antiparticle (antimeson) in which quarks are replaced by their corresponding antiquarks and vice versa. For example, a positive pion ($\pi+$) is made of one up quark and one down antiquark; and its corresponding antiparticle, the negative pion ($\pi-$), is made of one up antiquark and one down quark. Because mesons are composed of quarks, they participate in both the weak and strong interactions. Mesons with net electric charge also participate in the electromagnetic interaction. Mesons are classified according to their quark content, total angular momentum, parity and various other properties, such as C-parity and G-parity. Although no meson is stable, those of lower mass are nonetheless more stable than the more massive, and hence are easier to observe and study in particle accelerators or in cosmic ray experiments.[**24**]

2.4.1 Pions

In particle physics, a pion (or a pi-meson), denoted with the Greek letter pi: π is any of three subatomic particles: π^0, π^+, π^-. Each pion consists of a quark and an antiquark and is therefore a meson. Pions are the lightest mesons and, more generally, the lightest hadrons. Charged pions most often decay into muons and muon neutrinos, while neutral pions generally decay into gamma rays.[**25**]

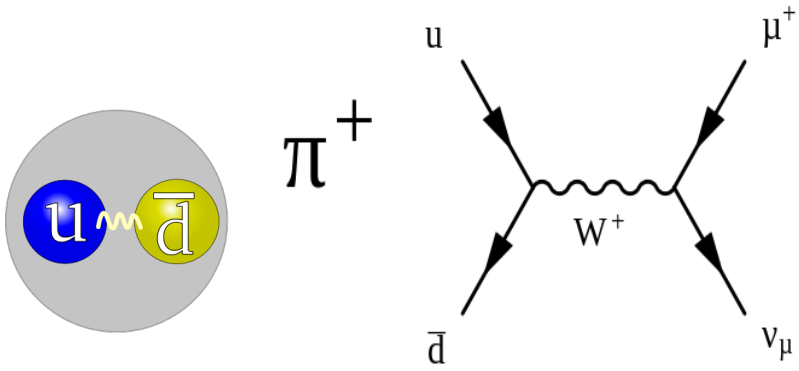

Figure 2.10: Quark structure of the pion and Feynman diagram of the dominant leptonic pion decay. Credit: Quora.

The pion can be thought of as one of the particles that mediate the interaction between a pair of nucleons. This interaction is attractive: it pulls the nucleons together. Written in a non-relativistic form, it is called the *Yukawa potential*. Pions, which are mesons with zero spin, are composed of first-generation quarks. The neutral pion π^0 is a combination of an up quark with an anti-up quark or a down quark with an anti-down quark. The two combinations have identical quantum numbers, and hence they are only found in superpositions. Together, the pions form a triplet of isospin. Each pion has isospin ($I = 1$) and third-component isospin equal to its charge

(Iz = +1, 0 or −1). The π± mesons have a mass of 139.6 MeV/c2 and a mean lifetime of 2.6033×10^{-8} s. They decay due to the weak interaction. The primary decay mode of a pion, with a branching fraction of 0.999877, is a leptonic decay into a muon and a muon neutrino:

$$\pi^+ \rightarrow \mu^+ + \nu_\mu \tag{2.1}$$

$$\pi^- \rightarrow \mu^- + \bar{\nu}_\mu \tag{2.2}$$

The second most common decay mode of a pion, with a branching fraction of only 0.000123, is also a leptonic decay into an electron and the corresponding electron antineutrino. This "electronic mode" was discovered at CERN in 1958.

$$\pi^+ \rightarrow e^+ + \nu_\mathrm{e} \tag{2.3}$$

$$\pi^- \rightarrow e^- + \bar{\nu}_\mathrm{e} \tag{2.4}$$

The π^0 meson has a mass of 135.0 MeV/c2 and a mean lifetime of 8.4×10^{-17} s. It decays via the electromagnetic force, which explains why its mean lifetime is much smaller than that of the charged pion.[**26**] The dominant π^0 decay mode, with a branching ratio of BR = 0.98823 , is into two photons:

$$\pi^0 \rightarrow 2\lambda \tag{2.5}$$

2.4.2 Kaons

Kaons have proved to be a copious source of information on the nature of fundamental interactions since their discovery in cosmic rays in 1947. They were essential in establishing the foundations of the Standard Model of particle physics, such as the quark model of hadrons and the theory of quark mixing. Kaons have played a distinguished role in our understanding of fundamental conservation laws: CP violation, a phenomenon generating the observed matter–antimatter asymmetry of the universe, was discovered in the kaon system in 1964.

There are 4 types of kaons:

- K$^-$, negatively charged (containing a strange quark and an up antiquark) has mass 493.7 MeV and mean lifetime 1.24×10^{-8} s.
- K$^+$ (antiparticle of above) positively charged (containing an up quark and a strange antiquark) must (by CPT invariance) have mass and lifetime equal to that of K$^-$. Experimentally, the mass difference is 0.032 MeV and difference in lifetimes is 0.11×10^{-8} s.

- K^0, neutrally charged (containing a down quark and a strange antiquark) has mass 497.7 MeV.
- $\overline{K^0}$, neutrally charged (antiparticle of above) (containing a strange quark and a down antiquark) has the same mass as K^0.

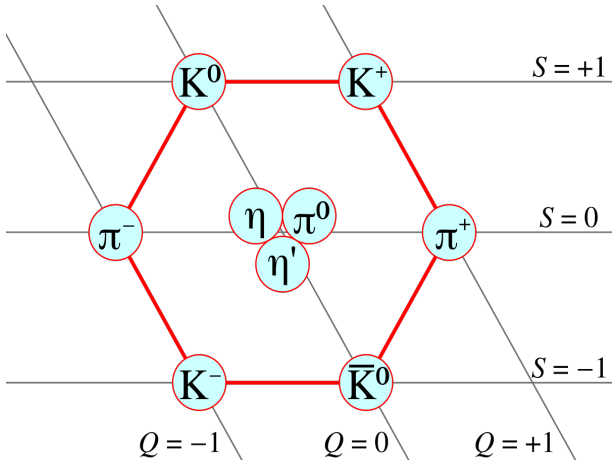

Figure 2.11: Combinations of one u, d or s quarks and one u, d, or s antiquark. Credit: physics.stackexchange.com.

Although the K^0 and its antiparticle $\overline{K^0}$ are usually produced via the strong force, they decay weakly. Thus, once created the two are better thought of as superpositions of two weak eigenstates which have vastly different lifetimes:

- The long-lived neutral kaon is called the K_L ("K-long"), decays primarily into three pions, and has a mean lifetime of 5.18×10^{-8} s.
- The short-lived neutral kaon is called the K_S ("K-short"), decays primarily into two pions, and has a mean lifetime 8.958×10^{-11} s.

The decay of a kaon (K^+) into three pions (2 π^+, 1 π^-) is a process that involves both weak and strong interactions.

Weak interactions : The strange antiquark ($\overline{s}$) of the kaon transmutes into an up antiquark ($\overline{u}$) by the emission of a W^+ boson; the W^+ boson subsequently decays into a down antiquark ($\overline{d}$) and an up quark (u).
Strong interactions: An up quark (u) emits a gluon (g) which decays into a down quark (d) and a down antiquark ($\overline{d}$).[**27**][**28**]

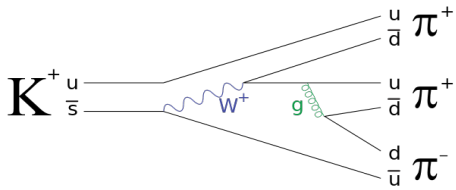

Figure 2.12: Kaon decay into three different pions. The decay requires both weak and strong interactions. Credit: News.softpedia.com.

Strangeness (S) is introduced to refine the understanding of the quark structure of matter. It has unraveled a new property of particles, a quantum number describing a large group of strongly interacting strange particles. The terms strange and strangeness predate the discovery of the quark, and were adopted after its discovery in order to preserve the continuity of the phrase; strangeness of anti-particles being referred to as $+1$, and particles as -1 as per the original definition. For all the quark flavour quantum numbers (strangeness, charm, topness and bottomness) the convention is that the flavour charge and the electric charge of a quark have the same sign. With this, any flavour carried by a charged meson has the same sign as its charge.[**29**]

2.5 Photographic nuclear emulsion

Photographic emulsion is not a true emulsion, but a insoluble light-sensitive colloid suspension which was used in film-based photography. Most commonly, in silver-gelatin photography, it consists of silver halide crystals dispersed in gelatin. The light-sensitive component is one or a mixture of silver halides: silver bromide, chloride and iodide. The halides arise from the reaction of common salt (sodium chloride (NaCl)), potassium bromide (KBr) and potassium iodide (KI) with silver nitrate. The emulsion is usually coated onto a substrate of glass, films (of cellulose nitrate, cellulose acetate or polyester), paper, or fabric.
However, the word emulsion is customarily used in a photographic context. The gelatin is used as a permeable binder, allowing processing agents (e.g., developer, fixer, toners, etc.) in aqueous solution to enter the colloid without dislodging the crystals. The light-exposed crystals are reduced by the developer to black metallic silver particles that form the image. Silver halides form crystal structures in which the elements are charged (Ag^+, Cl^-) = ion lattices. Theoretically, each silver ion is surrounded by six chloride ions (analogous to bromide and iodide) and each chloride ion is surrounded by six silver ions. In practice, however, at least some of the silver ions, so-called interstitial silver ions, leave their place and move around in the crystal. These ions play an important role in the further development of a latent image. Impurity silver halides are photosensitive, with the sensitivity decreasing from iodide to bromide to chloride. When a photo electron hits an interstitial silver ion, the two

combine to form the silver atom. If this process is repeated multiple times, a long-term stable and developable Ag_4 cluster is created. All sufficiently exposed crystals thus turn into metallic silver.
In order to make the images more distinctive and clear they are soaked in acidy developer liquid before being placed in a stop bath. The unexposed crystals are later removed from the layer during fixing, thus stabilizing the image. This process is performed in a darkroom with safe light filter lamps only. Thus the negative is created.[**30**][**31**][**32**]

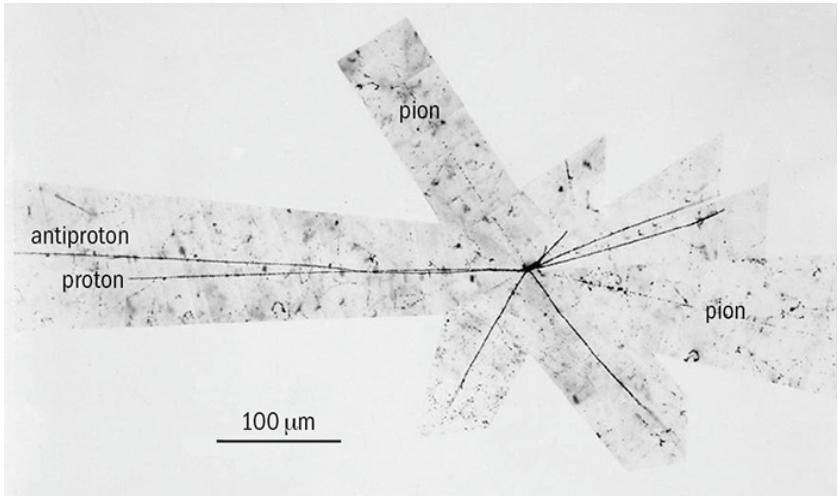

Figure 2.13: Nuclear emulsion decay capture. Secondary radiation decaying to further particles which leave identifiable lines. Credit: [**30**].

Colour films and papers have multiple layers of emulsion, made sensitive to different parts of the visible spectrum by different colour sensitizers, and incorporating different dye couplers which produce superimposed yellow, magenta and cyan dye images during development. A panchromatic emulsion is sensitive to light of any color or any wavelength of the visible electromagnetic spectrum. The spectral sensitivity extends over the entire visible range from 400 to 700 nm. This is achieved during the production of the emulsion by adding special light-absorbing substances (sensitization). Panchromatic films are characterized by a correct tonal reproduction of the colors: The perception of the gray levels corresponds to the impression of brightness of the eye. Black and white films for use in pictorial photography are therefore almost without exception panchromatically sensitized nowadays. An orthochromatic emulsion is sensitive to visible light plus ultraviolet, but without the color red. In addition, orthochromatic emulsions were often also used for so- called *speed plates* with a higher ASA or ISO values adding sensitivity. Orthochromatic or non-sensitized films and papers are mostly used where black and white is already used.

The early work was carried out with the type of emulsion used for conventional photography, which had a thickness of only a few microns. It was not until around 1930 that thick-layered emulsions (about 50 microns) were produced, first in research laboratories and later (1935–1937) on a commercial scale by Ilford Ltd in England. Ready coated, highly sensitive Q-plates, which are unusable for regular photogrpahy, aswell as K5 or L4 emulsions from the Ilford scientific product series are best known for use in the filed of hadron particle physics. These emulsions were exposed for some months at mountain altitudes, for example by Blau and Wambacher, and on subsequent examination 'stars' were found which were ascribed to the disintegration of nuclei in the emulsion caused by cosmic rays. By 1939, the technique was recognized as a useful tool for the investigation of nuclear and cosmic-ray phenomena, but it was considered to be only a qualitative method and of limited application. At the end of the war, Ilford produced a concentrated 'nuclear-research' emulsion containing eight times the normal amount of silver bromide per unit volume. It was in emulsions of this type exposed to cosmic rays at mountain altitudes that the pion was discovered by Powell and his colleagues in 1947.

2.5.1 Photographic dry plates

Many famous astronomical surveys were taken using photographic plates, including the first Palomar Observatory Sky Survey (POSS) of the 1950s. Glass-backed plates, rather than film, were generally used in astronomy because they do not shrink or deform noticeably in the development process or under environmental changes. Alternatively, tin plates, made from aluminum, were used, even though the dark background made contrast generation rather difficult. Larger exposure times were necessary in comparison to glass dry plates as glass is translucent. Finally, in the 1950s, first Kodak Ltd and then Ilford produced an emulsion capable of recording the tracks of particles moving with velocities such that they suffer the minimum possible energy loss (causing minimum ionization) in passing through the emulsion. Such emulsions are commonly known as *electron-sensitive emulsions*. The relatively small size and weight of emulsions enable them to be carried to great heights by means of free balloons. In this way, many studies have been carried out of a) the interactions of very energetic particles – energies greater than 50 GeV, b) the composition of the primary cosmic radiation and c) the development of the electron–photon cascade in the high atmosphere.[**33**]

CHAPTER 3

HAB-accountables

Any near space mission begins with the the flight body objective, in this case a weather balloon made from extremely elastic natural rubber and latex. It is either filled with helium, hydrogen or *balloon gas*[1]. As hydrogen is highly flammable, helium is often preferred as it is non-toxic, inert and does not burn.
Even in the 21st century, HAB-missions solely offer the possibility of recording meteorological measurements, such as the study of the vertical profiles of the atmosphere as well as conducting height-dependent research. Stratospheric balloons offer a relatively inexpensive and quickly available way of transporting larger and heavier scientific payloads to great heights. Another advantage is that the mechanical loads which occur during a balloon ascent are very low compared to, for example, rocket missions. This makes them interesting for a whole range of applications in research, the military sector, but also for training. For example, in preparation for manned space missions, NASA used balloon ascents to great heights in the stratosphere to test their astronauts' spacesuits. Similarly inspired experiments such as Felix Baumgartner's skydive in 2012 have also been carried out with the help of weather balloons.
In the following chapter sections, aspects regarding balloon systems, parachute and probes will be presented. These will set the basis for an inexpensive HAB-mission in heights of up to 38 kilometers above earth.

3.1 Prefabricated parts

The mission parts set-up is rather straight forward. A string of tear-resistant cord connects the weather balloon to a probe which, in turn, is also connected to a parachute. A schematic illustration is given below.
In comparison to basic party balloons which reach maximum heights of 3 km, balloons used by the German weather service are able to expand in increasing altitude while the ambient air pressure drops, thus allowing them to reach far superior heights. By doing so, they expand by factors of up to 12 times their original size. They are sold in different weight classes from 300 g to 3000 g, whereby higher weights obviously achieve higher payloads or altitudes. Manufacturers are, for example, Totex or K.K.S. from Japan. After the balloon has reached its maximum expansion and bursts, the probe starts to accelerate towards earth. In order to slow down the descent rate,

[1] Helium with at least 95% purity. Seven times lighter than air.

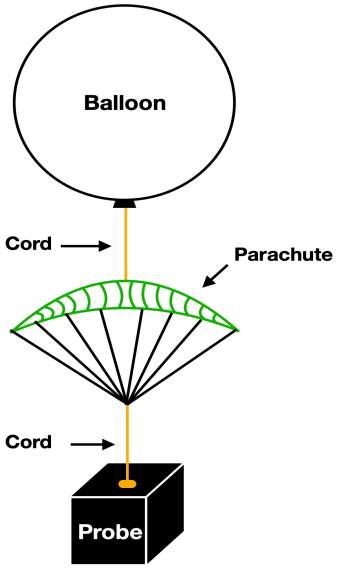

Figure 3.1: Illustration of a systematic set-up for a HAB-mission, including balloon, parachute and probe. Credit: William Roster.

a round canopy nylon parachute is used to decelerate the probe with increasing air resistance. After deploying, break force is applied to the string fixing the probe to the parachute. In order to maintain connection during ascent as well as descent, the string used must be able to withstand tearing. That is why the used string is able to withstand breaking loads of up to 200 N. However, it is illegal to use strings which are able to handle break loads exceeding 230 N. Of decisive importance is the size of the parachute, through which the descent speed can be regulated. As soon as the probe enters low altitudes ($\leq 5km$) the descent rate can not exceed 5 $\frac{m}{s}$. During steady descent in lower altitudes the approximation is made, that the drag resistance force equals the gravitational weight force.[**8**]

$$F_{\mathrm{G}} = F_{\mathrm{R}} \tag{3.1}$$

$$m \cdot g = \frac{1}{2} c_{\mathrm{w}} \cdot \rho_{\mathrm{L}} \cdot A_{\mathrm{proj}} \cdot v^2 \tag{3.2}$$

Here, m stands for the total mass, g 9.81 $\frac{N}{kg}$ for the acceleration due to gravity, c_w[2] is the shape-dependent drag coefficient, ρ_{L} is the air density, which at sea level is approximately 1.2 $\frac{kg}{m^3}$. With A_{proj}, the projected area, the size of the parachute is included in the calculation. Solving the equation for A_{proj} one obtains:

[2]The drag coefficient for round canopy parachutes is given as $c_w = 1.33$

$$A_{\text{proj}} = \frac{2m \cdot g}{c_{\text{w}} \cdot \rho_{\text{L}} \cdot v^2} \tag{3.3}$$

For a given payload of 1 kg for example, the projected surface area would have to be at least 0.5 m^2 in order to travel at speeds lower than 5 $\frac{m}{s}$. Therefore a round canopy parachute would have to have a diameter of at least 80 cm.
While allowing enough string to recover the probe in case it is stuck in an elevated position, the maximum length of 60 m must not be exceeded.
The probe itself consists of a styrofoam box. EPS is light weight, cheap and easily adaptable to fit any necessary needs. It is able to absorb energy upon impact and also offers good insulation against temperature fluctuations, both of which help to protect the sensitive electronic devices stored within the probe. As electronic devices only work within a certain temperature margin, the use of warm pads can be helpful when trying to maintain a certain temperature in the otherwise air sealed probe, as ambient temperatures reach below -55 °C. The volume should range from 3-5 L, allowing enough space for all necessary technological devices to be stored. Additionally further styrofoam walls can be implemented, which are helpful in distributing the force acting upon the string connected to the probe. Such styrofoam walls can also be connected to the outside of the probe preventing it from spiraling when confronted with cross winds. That way, the on-board camera produces better results.
When retrieving the probe, GPS-GSM based trackers are used to transmit coordinates. However GSM connection is designed for urban use, implying that its range is based on near-ground reception. Reliable alternatives to GSM are SATCOM or radio transmissions.

3.2 Legal actions

HAB-missions can generally be categorized in 3 consecutive phases, each of which brings its own challenges. These comprise of an official registration at the according air office control, including upholding a time and area slot and retrieving the probe. As laws regarding all 3 phases are in place, legal considerations will be made for each of them. This way, the legally binding process of how to properly design, plan and execute a HAB-mission is explained in step by step instructions. [**34**]

3.2.1 Take-off preparations

The framework of this mission is linked to a free air balloon of the class ”light”. This means the sum of all probes must not exceed a maximum total weight of 4 kilograms. This being said, each probe must not weigh more than 3 kilograms. Such aviation objects are subject to approval by the according European state. The legal basis is set by the European Commission and can be looked up under the *Implementing Regulation* nr. 923/2012, subsection ”SERA.3140 Unmanned free air balloons”. These

regulations also cover balloon missions of the categories *intermediate* and *heavy*. The approval is given by the air office of the respective federal state or, if the balloon ascent is to take place near an airport, the DFS.[**35**]
The main purpose of the DFS is to check whether the mission is allowed to take off from the requested coordinates. As the town of Giessen falls within the jurisdiction of the ICAO VFR region of Frankfurt, take-off coordinates inside the controlled air space class D are not prohibited. Any take-off in this area presents a potential risk for the heightened density of aircraft surrounding Frankfurt airport.

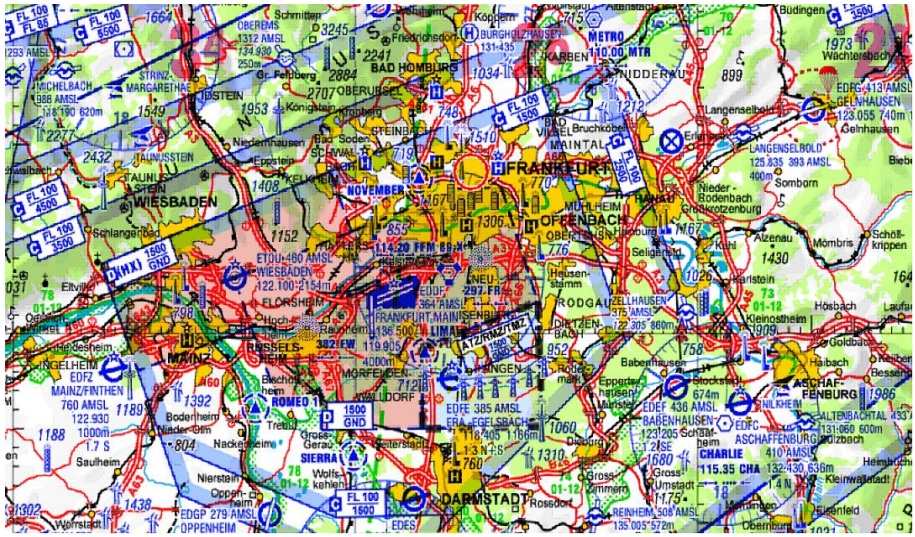

Figure 3.2: VFR map of the airspace in the vicinity of Frankfurt. Credit: ICAO.

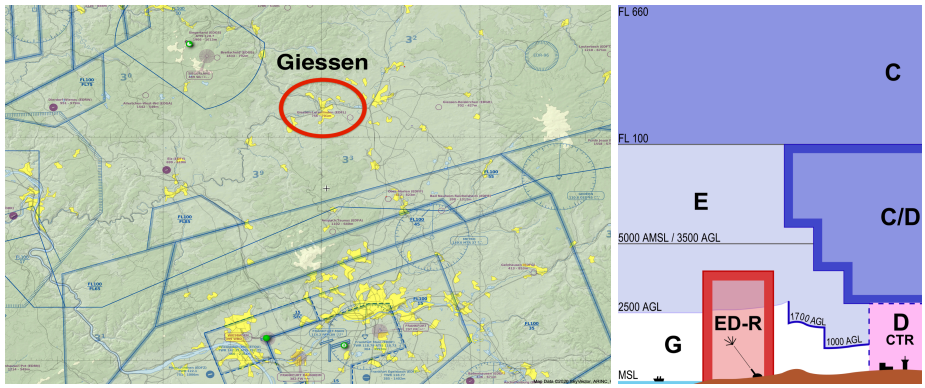

Figure 3.3: Map identifying Giessen in air space class C, Credit: Skyvector.com.

As can be seen above, Giessen is isolated in the regard of controlled air space. Thus coordinates in this region are not hazardous. Also it is extremely unlikely for the balloon to reach the closest controlled air space, marked class C, in an altitude lower than 5500 feet. This is due to the fact that the the channel of the jet-stream west wind, which gives the balloon its horizontal speed, is located between 8 and 15 kilometers above ground. Thus the balloon will have exceeded altitudes of controlled air space before gaining velocity and coming into the vicinity of any airport activities.

The aviation application must take place no later than two weeks before the planned start date. Information regarding:

- insurance
- starting date and coordinates in latitude and longitude
- starting time (UTC)
- probe design and payload
- total weight
- total elongation
- ascent and descent rate [$\frac{feet}{min.}$]
- flight duration
- colour

needs to be included.[**36**] Air traffic control then issues a navigation warning (NOTAM) notifying all aircraft in the area if necessary. Additionally the balloon ascent must be insured by a special private aviation owner's liability insurance.
The key message of the legal obligation can be summarized as follows: *"An unmanned free balloon may only be operated if people or property are not endangered when the balloon or part of it, including the payload, hits the surface of the earth."* (European Commission, 2012, Annex 2, Section 2.2.5). As mentioned above the insurance certificate of an established provider company must be attached to the formal request forwarded to the respective air traffic control office.
In any case, it must be ensured that the surface density does not exceed 13 $\frac{g}{cm^2}$. In this case a 6 L probe with a surface area of 2200 cm^2 would allow for a maximum weight six times over the legal 4 kg of mission class "light". If all regulations have been complied with, insurance has been taken out and the flight has been registered with the Aviation Office or DFS, nothing stands in the way of taking off.

3.2.2 Launch & flight

Before flight takes place, the anticipated flight path should be cross-checked and simulated, taking into account the current weather situation and prediction. Online tools such as the Spaceflight Landing Predictor[3] (SLP) developed by researchers from the University of Cambridge, use weather data from NOAA. Their accuracy depends, in addition to the quality of the weather forecast, which cannot be influenced by the user, also on how precisely the ascent and descent rates of the balloon are known.

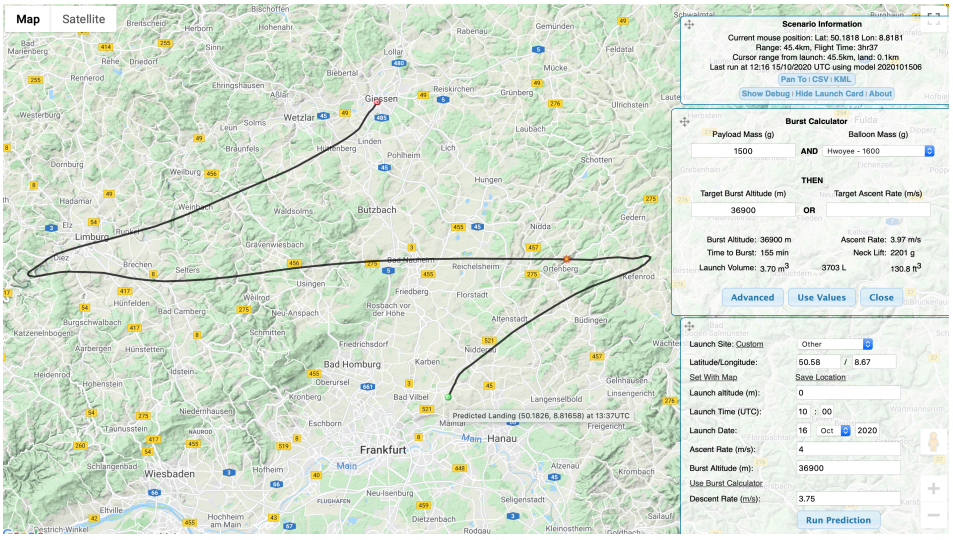

Figure 3.4: Spaceflight Landing Predictor display of exemplary HAB-flight under use of the *"Burst calculator"* Credit: University of Cambridge.

Additional tools, such as the *burst calculator* also allow for the user to calculate the desired burst altitude or ascent rate by supplying information regarding payload and balloon mass. Some weather conditions, such as the presence of strong winds, make the launch of a balloon very difficult to achieve. In addition, free balloons may only be launched with a horizontal visibility of at least 5 km and a cloud cover of a maximum of $\frac{4}{8}$. Finally the contact details (name, mobile number, address, email address) of the people responsible for the balloon must be applied clearly visible and waterproof on the probe. The start must take place at the time agreed with the responsible air authority. As the time slot application must take place 2 weeks in advance of take-off, one can hardly tell if the weather conditions will be suitable or not. In later case one must either apply for a second launch date or is provided with such by the air traffic control office. In addition air traffic control offers a window of several days for take-off if the weather forecast implies a denial for launch to commence.

[3] http://predict.habhub.org/

3.2.3 Probe retrieval

GSM-based communication is used to transmit GPS coordinates in order to locate the probe after landing. Since the transmission masts of the cellular network have a relatively flat radiation pattern, cellular reception is almost impossible in altitudes exceeding 3 km, leading to radio silence for a majority of in-flight time. On-board data logging devices however, are able to register and save real time GPS-coordinates which allow a reconstruction of the flight path after securing the memory card. Luckily the previously introduced SLP allows users to head to the previously calculated landing point shortly after take-off. Since Europe is in a westerly wind zone, the landing points of the probes here are mostly to the east of their starting point. Under typical weather conditions, the mean distance between the take-off and landing point of a stratospheric balloon is around 100-200 km.[**8**]

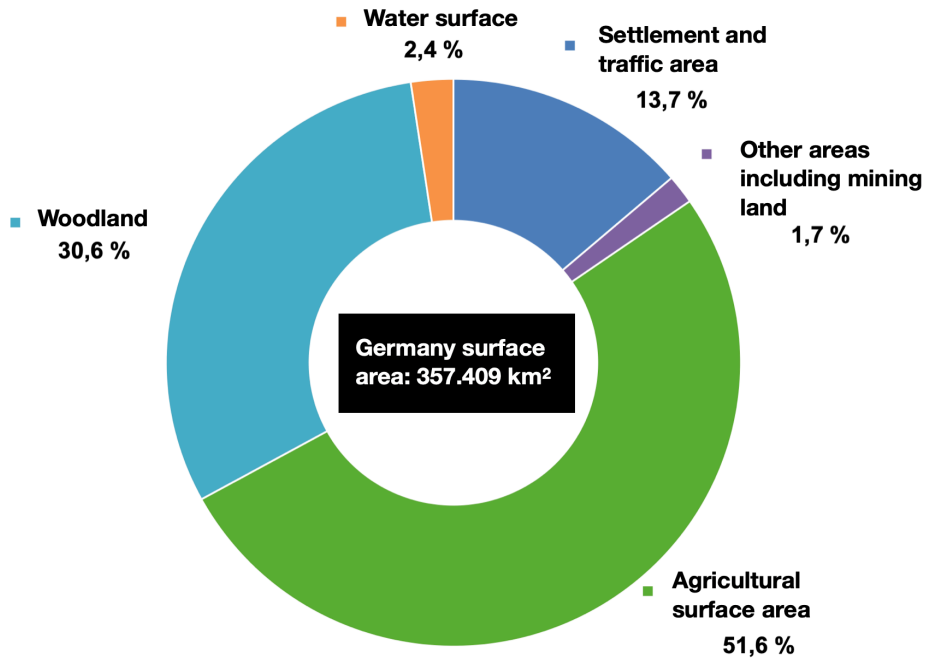

Figure 3.5: Pie chart illustrating the individual divided percentages of german surface area in regard of potential landing terrain. Credit: [**8**].

In Germany, settlement and traffic areas account for around 14%. Therefore it is not unlikely that the payload will land in a populated area. On the other hand, however, over half of Germany's area consists of agricultural land and around a third is forested. So it is much more likely one is confronted with a forest related landing during the rescue than the probe landing on a settlement area.

Of the unfavorable country scenarios, a tree landing is the most likely. This is partially why the cord connecting probe and parachute stretches 10 m. In case of the parachute actually getting stuck in a tree top 10 or less meters above ground, the probe should still be retrievable. With a little luck, however, the probe will also hit open terrain. A quadrocopter with a camera can assist with large-scale searches.

CHAPTER 4

Mission preparation

The following chapter deals in detail with the components used, their specifications and application settings. This includes both, the parts used to set up and design the flight object as well as the electronic devices used for measurements within the probe. Furthermore, all experiment-specific aspects that have to be taken into account in relation to executing the mission are addressed. Lastly the flight specific settings will be determined in regard to the HAB-mission equipment corner stones.

4.1 Framework physics

The mission relocation is primarily linked to the successful implementation of the on-board experiment. In this case the mentioned implementation concerns the targeted measurement of kaons within the cosmic showers of earth's atmosphere. Since kaons can only be detected above a certain minimum height, it is important to let the probe penetrate as far into the stratosphere as possible. At altitudes of a few kilometers and higher, certain physical framework conditions arise. These include temperature and pressure fluctuations throughout flight which need to be taken under consideration. Therefore each component must be chosen and set-up in according manor to fit the described conditions.

4.1.1 Flight calculation

As previously mentioned, the maximum total weight of the flying object must not exceed 4 kg. It should now be taken into account that both the balloon and the parachute have their own weight. This dead weight is inevitably related to the total weight of the probe but also to the degree of feasibility of the experiment. The heavier the individual parts, the greater the maximum height achieved. Bigger parts also allow for bigger payloads, with the weight of the component equalling the payload. This effectively means they cancel each other out. Ultimately one needs to weigh up which components are best suited to use in the according constellation. As highlighted in 4.1 the choice for this mission was made in favour of a class 1600 balloon and class 2500 canopy parachute. In addition, including a connection cord, these parts weigh approximately 1700 g, thus allowing the probe to weigh a maximum of approximately 1500 g. Both of these components can be seen further below.[**37**]

Component	Weight [g]	Payload(max.) [g]	Burst altitude [m]	Diameter [cm]
Balloon	800	800	30000	-
””	1600	1600	36000	-
””	2000	2000	38000	-
Parachute	70	800	-	107
””	80	2500	-	130

Table 4.1: Component information from different mission parts. Credit: [**37**].

Based on this assumption the next key aspect, the target burst altitude, can be established based on online tools such as the *helium-calculator* which can be seen in figure 4.1. This tool either takes a target burst altitude or target ascent speed. With a probe weight of 1500 g for example, the desired burst altitude of roughly 37 km may be achieved with an ascent rate of just under 4 $\frac{m}{s}$. This requires 3700 L of Helium, which equals less than half of a 50 L bottle at 200 bar inside pressure. Commonly the rule of the thumb when calculating the amount of helium needed is:

$$Helium[l] = Balloonweight[g] + 1.5 \cdot payload[g] \tag{4.1}$$

In this case, a class 1600 balloon carrying 1500 g of payload would require 3850 liters. Obviously one can always fill the balloon with more helium, making it rise faster but therefore reaching a lower altitude.

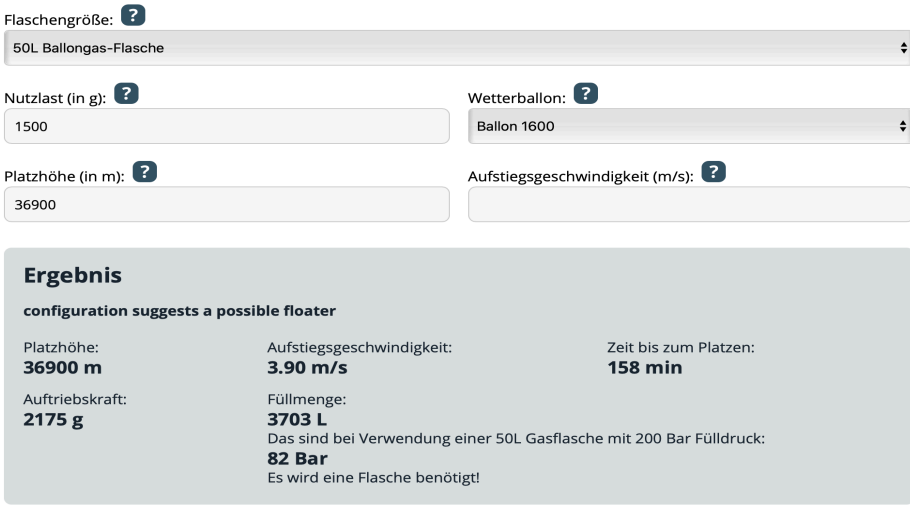

Figure 4.1: Helium calculator used to establish the required amount of Helium for simulated varying conditions. Credit: [**37**].

More helium means more expansion volume in the balloon which makes the balloon burst sooner. Under these take-off conditions the balloon would take exactly 150 minutes to burst. This information can now be used in turn to feed into the SLP.

Figure 4.2: Natural rubber/latex-mix class 1600 balloon. Credit: [**37**].

Figure 4.3: Nylon canopy class 2500 parachute. Credit: [**37**].

The class 2500 canopy has a diameter of 130 cm. With a payload of 1500 g the descent rate is calculated at:

$$v = \sqrt{\frac{2m \cdot g}{c_{\mathrm{w}} \cdot \rho_{\mathrm{L}} \cdot A_{\mathrm{proj}}}} = 3.73 \frac{m}{s} \tag{4.2}$$

If the descent rate were of linear nature this would mean the probe would take 9920 seconds, or 165 minutes to descent from an altitude of 37 000 meters. However the canopy break force increases with air pressure, implying that the descent speed curve is one of parabolic nature. At an ascent rate of 4 $\frac{m}{s}$ the SLP calculates the balloon to require 3h37 minutes to reach an altitude of 37 kilometers and descent down back to earth reaching a minimum speed of 3.75 $\frac{m}{s}$ when approaching altitudes of 5 kilometers and less. When subtracting the ascent time from the total flight duration the descent time is predicted to be just 64 minutes. Therefore the average descent speed is 9.61 $\frac{m}{s}$. From this parabolic average the maximum descent speed results in approximately 22 $\frac{m}{s}$ or 80 $\frac{km}{h}$ as the ambient pressure drops to 0.01 bar. If ascent and descent are summed up, the flight duration would result in just over 3.5 hours. This information can come in useful when configuring the on board electronic devices and according battery life.

4.2 Research parameters

Essential electrical devices for such a balloon mission are obviously an outward facing camera, sensors to measure the altitude and the atmospheric characteristics such as pressure, atomic abundances and temperature. Also the probe should be able to measure ascent and descent rate as well as the time responsive GPS coordinates so that the exact flight path can be reconstructed after the probe has landed safely.
In this project, the probe additionally carries high-sensitive photo emulsion coated glass plates which are supposed to decelerate and encapture a Kaon or its decay. The experimental research carried by the probe can therefore be divided into analog and digital measurements.

4.2.1 Electrical devices

The camera which is fitted inside the probe wall is the *apeman action cam 79*. Throughout flight the action cam will be recording at 1080 FHD/ 60 FPS. As the camera battery will suffer under the low ambient temperatures it will be connected to a external battery pack to prevent the camera from turning off before end of flight. All other measurements mentioned above will be carried out by the *Stratoflights Datenlogger*. This device is equipped with all necessary hardware, such as the sensors as well as the micro controller which converts analog readings into digital values. The controller itself will be fixated within the probe whereas the sensors will be led through the probes wall, similar to the camera lens. The in-flight readings are saved on the integrated memory device and can be analyzed and plotted after the probe has been secured. The data observed includes:

- altitude
- GPS
- velocity
- temperature (inside and outside)
- humidity
- pressure

Furthermore a second controller, the *Arduino one* is placed within the probe. It features a further data stacking module as is measures and records the ambient ozone density. By setting a critical density value, the ozone readings can be cross referenced with the according altitudes to establish the location and thickness of the ozone layer in the VFR area of Frankfurt.

4.2.2 Non-electrical devices

4x2 inch Q-plates have specially been manufactured on request by *Ilford photo* UK. This production is inevitable as average photographic photo plates or emulsions do not meet the specific requirements necessary to detect cosmic ray particles. Isolated from any light, they are placed within a sealed box, which itself is placed inside the probe. This way the light sensitive plates are undeveloped before they enter the upper atmosphere. The extra safety precausion also helps to prevent damage to the glass plates during landing. Afterwards the plates need to be developed under a plate specific, wavelength sensitive dark room lamp, such as the Ilford SL1 or DL20. Additionally the lamp needs be equipped with a filter, such as the Ilford 904 or, if 904 is not available, the 902 model.[**38**][**39**]

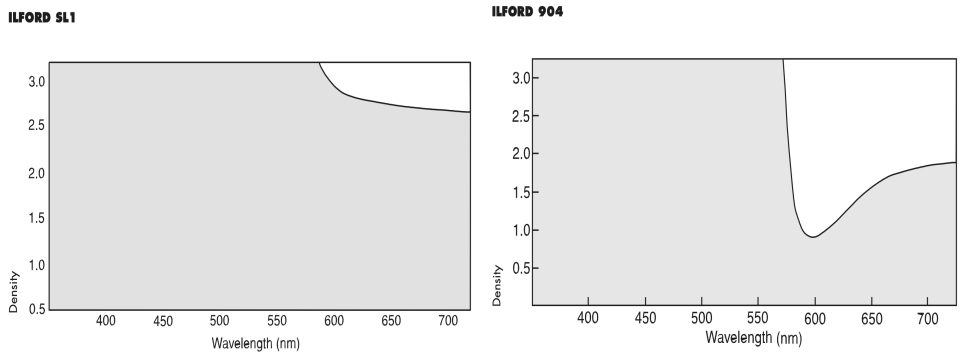

Figure 4.4: Characteristic wavelength sensitivity of the SL1 safe light. Credit: Ilford Photo.

Figure 4.5: Specific wavelength sensitivity of the 904 safe light filter. Credit: Ilford Photo.

After exposure Ilford Phenisol should be used as developer. This is a non-caustic developer supplied as a liquid concentrate. It should be diluted 1+4 with water for use. The recommended development time at 20°C is 4 minutes, with continuous agitation. However, if not available, the self-mixable developer ID-72 or ID-13 are sufficient. Both of which can be found in the Q plates data sheet. Q plates should be fixed in fresh fixer for twice the time it takes for the plates to clear, then washed in a good supply of running water for about 8 minutes. A final rinse to which a few drops of Ilford IlfotolL wetting agent has been added will aid rapid and uniform drying. After developing, the remaining metallic silver needs to be fixated for twice the time it takes for the plates to clear. The factory recommends using Ilford Hypam fixer. To finish, the plates need to be washed in a good supply of running water for about 8 minutes. This process clears all prior used chemicals. A final rinse to which a few drops of Ilford Ilfotol wetting agent has been added will aid rapid and uniform drying.

Figure 4.6: Developer (left): Phenisol, Washer (middle): Ilfotol and Fixer (right): Hypam. All products are necessary to handle the exposed Q-plates. Credit: Ilford Photo.

As the plates are a very extra and rarely used product the according products for proper treatment are limited. Thus working with purely Ilford products is a sensible choice since it would be a shame to ruin the plates after exposure. If exposure and development are successful, small linear lines or radial symmetric decays bursts should be visible under a microscope. The characteristics of such lines, i.e. the length and width give insight into which particle has been captured.

CHAPTER 5

Experimental Analysis & Evaluation

The HAB-mission was successfully executed on the xxth October 2020. All readings and experimental measurements acquired during flight can now be analysed and displayed in a graphical manor. To do so, the in 4.21 and 4.22 before mentioned data will be plotted for visualization using multiple software gadgets. At the end of this chapter the experimental results will be evaluated under the background of common scientific knowledge.

5.1 Data assessment

5.1.1 Flight characteristics

speed, Gps, altitude etc.

5.1.2 Vicinity conditions

temp, humidity, pressure,

5.1.3 Ozone layer

Determination of bottom border, critical value(ppm)

5.2 Nuclear emulsion

5.2.1 Post-flight development

5.3 Quality review

CHAPTER 6

Conclusion & Summary

Evaluation and Assessment looking back. Improvements ?

APPENDIX A

Camera footage

APPENDIX B

C-script: O_3-data

B.1 Arduino Code

The following C-script is used to generate the readings discussed in chapter 5.1.3. Credit: Tim Oelke, Lars Klingenstein, Noria Brecher

```
#include <DFRobot_OzoneSensor.h>
#include <Seeed_BME280.h>
#include <SPI.h>
#include <SD.h>
#include <Wire.h>
#include "RTClib.h"


#define COLLECT_NUMBER   20              // collect number, the collection
    range is 1-100
#define Ozone_IICAddress ADDRESS_3
/*   iic slave Address, The default is ADDRESS_3
       ADDRESS_0               0x70      // iic device address
       ADDRESS_1               0x71
       ADDRESS_2               0x72
       ADDRESS_3               0x73
*/


const int chipSelect = 10; //10 is default by shield, but normally on Pin 4


DFRobot_OzoneSensor Ozone;
BME280 bme280;
RTC_DS1307 rtc;


void setup() {
  Serial.begin(9600);
  delay(3000);
  Serial.println("Initializing SD card...");
  if (!SD.begin(chipSelect)) {
    Serial.println("SD Card error");
    return;
  }
  Serial.println("card initialized");
  if (!rtc.begin()) {
```

```
37      Serial.println("No RTC found");
38    } else {
39      Serial.println("RTC clock found");
40    }
41    if (!rtc.isrunning()) {
42      Serial.println("RTC is not configured");
43    }
44
45    if(!Ozone.begin(Ozone_IICAddress))
46    {
47      Serial.println("I2c device number error!");
48      delay(1000);
49    }
50    else{
51      Serial.println("I2c connect success!");}
52  /*   Set iic mode, active mode or passive mode
53         MEASURE_MODE_AUTOMATIC            // active  mode
54         MEASURE_MODE_PASSIVE              // passive mode
55  */
56      Ozone.SetModes(MEASURE_MODE_PASSIVE);  // MUSS GGF NOCH UMGESTELLT
            WERDEN!
57
58      if(!bme280.init()) // Wenn keine Daten vom BME abgefragt werden können
            ...
59          {
60            Serial.println("FEHLER beim BME!"); // ...dann soll eine
                  Fehlermeldung ausgegeben werden.
61          }
62  }
63
64
65  void loop() {
66
67      write_all_data(get_time(), String(bme280.getTemperature()), String(
            bme280.getPressure()), String(bme280.getHumidity()), String(Ozone.
            ReadOzoneData(COLLECT_NUMBER)));
68      Serial.println("");
69      delay(5000);
70  }
71
72
73  String get_time() { //Read Time from RTC
74    String timestring;
75    DateTime now = rtc.now();
76    /*
77    timestring = now.day();
78    timestring += "-";
79    timestring += now.month();
80    timestring += "-";
81    timestring += now.year();
82    timestring += " ";
83    */
84    timestring += now.hour();
85    timestring += ":";
86    timestring += now.minute();
```

```
87    timestring += ":";
88    timestring += now.second();
89    Serial.println(timestring);
90    return(timestring);
91  }
92
93  void write_all_data(String timestring, String temp, String pressure, String
        humidity, String ozone) {            //Write Temp to SD card
94    String dataString = timestring + "; " + temp + "; " + pressure + "; " +
          humidity + "; " + ozone;
95    File dataFile = SD.open("Data.txt", FILE_WRITE);
96    if (dataFile) {
97      dataFile.println(dataString);
98      dataFile.close();
99      Serial.println(dataString);
100   }
101   else {
102     Serial.println("error writing Data.txt");
103   }
104 }
```

.

APPENDIX C

Acronyms

AGN Active Galactic Nuclei

ASA American Standards Association

DFS Deutsche Flugsicherung (German air traffic control)

EAS Extensive Air Showers

EM Electromagnetism

EPS Expanded Polystyrene

FST Fermi Space Telescope

GPS Global Positioning System

GSM Global System for Mobile Communications

HAB High-altitude balloon

HZE High (H), atomic number (Z), energy (E)

ICAO International Civil Aviation Organization

ISO International Organization for Standardization"

ISS International Space Station

LHC Large Hadron Collider

NASA National Aeronautics and Space Administration

NOAA National Oceanic and Atmospheric Administration

NOTAM Notice(s) to Airmen

POSS Palomar Observatory Sky Survey

SATCOM Satellite Communication

SLP Spaceflight Landing Predictor

UHECR Ultra-high-energy cosmic rays

UV Ultra-violet

VFR Visual Flight Rules

List of Figures

List of Tables

Bibliography

[1] https://www.space.com/32644-cosmic-rays.html

[2] https://www.swpc.noaa.gov/phenomena/galactic-cosmic-rays

[3] https://physicstoday.scitation.org/doi/abs/10.1063/PT.3.1437?journalCode=pto

[4] https://imagine.gsfc.nasa.gov/science/toolbox/cosmic-rays1.html

[5] https://www.mpi-hd.mpg.de/hfm/HESS/public/hessbio.html

[6] https://astronomy.swin.edu.au/cosmos/c/cosmic+ray+energies

[7] https://iopscience.iop.org/article/10.1088/1367-2630/12/7/075009

[8] https://www.vox.com/the-highlight/2019/7/16/17690740/cosmic-rays-universe-theory-science

[9] https://agupubs.onlinelibrary.wiley.com/doi/pdfdirect/10.1002/2016SW001410

[10] https://www.nationalgeographic.org/encyclopedia/atmosphere-RL/

[11] https://www.space.com/17683-earth-atmosphere.html

[12] https://scied.ucar.edu/shortcontent/earths-atmosphere

[13] https://www.sattec.org/stratosphaerenmissionen/leitfaden-stratosphaerenballon/stratosat-leitfaden.pdf

[14] M. Bagshaw, P. Illig. *The aircraft cabin environment*, in Travel Medicine (Fourth Edition), 2019.

[15] R. Gifford, *International Encyclopedia of the Social & Behavioral Sciences*, 2001.

[16] https://www.hep.physik.uni-siegen.de/pubs/diss/kickelbick-dr.pdf

[17] https://indico.cern.ch/event/318730/attachments/613330/843782/Cosmic-Radiation-LessonPlans.pdf

[18] http://www.antarcticglaciers.org/glacial-geology/dating-glacial-sediments-2/cosmic-rays/

[19] S. Käs. *Multiparameter Analysis of the Belle II Pixeldetector's Data*, 2019.

[20] K. Dort. *Search for Highly Ionizing Particles with the Pixel Detector in the Belle 2 Experiment*, 2019.

[21] W. Roster. *Design of a CNN to establish location and mass of dark matter distribution by means of weak gravity lensing*, 2020.

[22] https://www.britannica.com/science/meson

[23] http://www.thingsmadethinkable.com/item/mesons.php

[24] http://www.personal.soton.ac.uk/ab1u06/teaching/phys3002/course/20-PCCP.pdf

[25] http://hydrogen.physik.uni-wuppertal.de/hyperphysics/hyperphysics/hbase/particles/hadron.htr

[26] https://www.taborelec.com/pion-decay-solution-note

[27] https://phys.org/news/2019-09-ultra-rare-kaon-evidence-physics.html

[28] http://hyperphysics.phy-astr.gsu.edu/hbase/Particles/kaon.html

[29] L.B. OKUN. *Leptonic decays of K-mesons and hyperons*, in Leptons and Quarks, 1984.

[30] https://cerncourier.com/a/nuclear-emulsions/

[31] http://gymarkiv.sdu.dk/MFM/kdvs/mfm2030-39/mfm-30-3.pdf

[32] http://stratocat.com.ar/stratopedia/427.htm

[33] https://www.ilfordphoto.com/amfile/file/download/file/1855/product/579/?store=ilfordbrochure fromstore=ilford-uk

[34] https://www.easa.europa.eu/sites/default/files/dfu/Easy20Access20Rules20for20Standardised20E

[35] https://www.dfs.de/dfs-homepage/de/Flugsicherung/Safety/Sicherheitsmanagement/

[36] https://rp-kassel.hessen.de/planung/verkehr/luftverkehr

[37] https://www.stratoflights.com/shop/

[38] https://www.ilfordphoto.com/amfile/file/download/file/1858/product/758/

[39] https://www.ilfordphoto.com/amfile/file/download/file/605/product/614/